UNCLASSIFIED

AD 258 201

Reproduced
by the
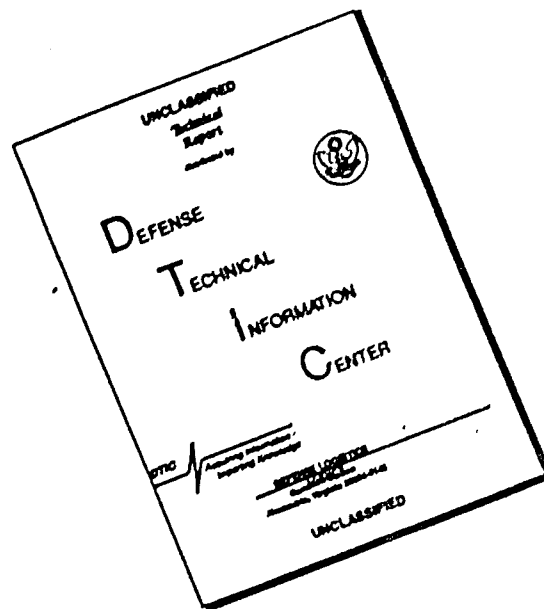
ARMED SERVICES TECHNICAL INFORMATION AGENCY
ARLINGTON HALL STATION
ARLINGTON 12, VIRGINIA

UNCLASSIFIED

DISCLAIMER NOTICE

THIS DOCUMENT IS BEST QUALITY AVAILABLE. THE COPY FURNISHED TO DTIC CONTAINED A SIGNIFICANT NUMBER OF PAGES WHICH DO NOT REPRODUCE LEGIBLY.

41-3-4
XEROX

449300

METALLURGY

DEPARTMENT OF METALLURGY

Institute of Metals and Explosives Research

UNIVERSITY OF UTAH
SALT LAKE CITY, UTAH

MEASUREMENTS OF SHOCK AND DETONATION PRESSURES

M. A. Cook, R. I. Keyes and W. O. Ursenbach

Technical Report
Contract NOw 61-0411-d

April 28, 1961

Project Director: M. A. Cook

MEASUREMENTS OF SHOCK AND DETONATION PRESSURES

ABSTRACT

An "aquarium technique" for the measurement of shock and detonation pressures
is described which is capable of measuring accurately pressures over a range
extending from roughly one to several hundred kilobars. An experimental deter-
mination of the equation of state for water, upon which use of the aquarium
technique relies, is presented and compared with results obtained by other
investigators. Similar data are presented for lucite. Measurements of pressures
at the detonation front for a variety of explosives including both ideal and non-
ideal ones are presented for various charge diameters and lengths using explosives
of widely different reaction zone lengths. These pressures were found to cor-
respond to the Chapman-Jouguet value of the detonation pressure calculated from
thermohydrodynamic theory.

Introduction

When a shock wave propagates through an undisturbed medium of density ρ_1, all the remaining shock wave parameters may be expressed uniquely in terms of any one chosen parameter. For example, pressure, temperature, and particle velocity may each be expressed uniquely in terms of the velocity of the shock wave. The fact that disturbances, even of relatively low pressure, propagate in water as shocks, coupled with the fact that water is transparent, thereby permitting convenient and continuous observation of shock velocity by a streak or framing camera, suggest that pressures of shock in an incident medium may be measured by transmitting them into water.

Before water can be used as a pressure measuring medium, however, its shock parameters must be known. The Rankine Hugoniot curves for water have been derived by a number of investigators including Kirkwood and Montrall,[1] Kirkwood and Richardson,[2] Richardson, Arons and Halverson,[3] Arons and Halverson,[4] and Doering and Burkhardt.[5] In these treatments systematic extrapolations of Bridgman's[6,7] PVT data for water were made. Probably the most comprehensive extrapolation of Bridgman's PVT data, however, was carried out by Snay and Rosenbaum[8] who used more recent data of Bridgman[9,10] which for water extended to 36,500 kg/cm^2 and for ice VII to 50,000 kg/cm^2.

A different approach was used in a later study by Walsh and Rice.[11] In their method an intense plane shock wave was generated in an aluminum plate by the detonation of a slab of Composition B in contact with one side of the plate. The shock through a portion of the plate was then transmitted into water. Higher pressures in the aluminum plate were reported by "slapping" the aluminum plate with a thin, high velocity, explosively driven plate rather than detonating the charge directly in contact with the test aluminum. By application of a special streak camera technique pioneered by Walsh and coworkers and through use of a previously derived equation of state for aluminum the shock velocity in water as a function of the corresponding shock pressure in the aluminum at the interface was determined. Continuity conditions of pressure and particle velocity across the interface between the aluminum and water were then applied to determine the Hugoniot curves for water.

In determining shock parameters for water a factor which should be considered is the possibility of a phase change of the medium within the shock wave. This possibility was investigated by Snay and Rosenbaum[8] and by Walsh and Rice.[11] According to Snay and Rosenbaum the Rankine Hugoniot curve for supercooled water and the Rankine Hugoniot curve for partially frozen water are never far apart, and thus the shock velocity would not be materially affected if freezing did occur. Since partial freezing of a liquid should lead to reduced transparency, because of differences in indices of refraction of water and ice, Walsh and Rice carried out some transparency experiments of water being traversed by a shock wave in the pressure range of 30 to 100 kilobars. No sign of opacity due to freezing was observed. They concluded, therefore, that even though P,T conditions might be proper for freezing under static conditions the time the liquid was under the correct conditions within the shock wave apparently was too short for freezing to occur.

In using water as a pressure gauge (by observing the transmission of the shock into it) one must calculate from the measured shock pressure in water the pressure in the incident medium from which the water shock was transmitted. In a previous application of the "aquarium technique" for the measurement of pressure, two procedures were used to perform such a calculation.[12] The first method, which was considered the more exact one, was patterned after a treatment given by Riemann for a shock propagating across a boundary into a medium of lower impedance. The second method utilized the shock "impedance mismatch" equation

$$P_i = \frac{P_t(\rho_t V_t + \rho_i V_i)}{2\rho_t V_t} \tag{1}$$

where p is the pressure, ρ is the initial density of the medium before being traversed by a shock, V is the velocity of the shock, and subscripts i and t designate the incident medium and the transmitting medium, respectively. Although the shock impedance mismatch equation theoretically should only be accurate when the wave reflected at the interface is a weak shock, in the investigations covered by Reference 12, where the reflected wave was a rarefaction, equation (1) was found to yield results in a very good agreement with the first method. Consequently, in the present study equation (1) was used to

calculate p_i from measured values irrespective of whether the reflected wave
was a release wave or a shock wave.

This report presents results obtained by application of the aquarium method
for the measurement of detonation pressures of a number of explosives.

Furthermore, since the results of Snay and Rosenbaum were derived from an
extrapolation of low pressure PVT data, and since the curve of Walsh and Rice
is dependent upon the equation of state of aluminum and application of continuity
conditions across the aluminum-water interface, results of a shock parameter study
for water by a third, independent method are described. Less comprehensive results
are also presented for lucite which, like water, possesses desirable character-
istics for use as the transmitting medium for measurement of pressure.

Experimental

(a) Shock parameter determinations

The shock parameters which are of interest in this study are related by the
familiar hydrodynamic equations

$$p - p_o = \rho_1 VW \tag{2a}$$
$$W/V = [1-(\rho_1/\rho)] \tag{2b}$$

and the approximate relation

$$W \doteq V_{fs}/2 \tag{3}$$

where p is the pressure, ρ is the density, V is the shock velocity, V_{fs} the
free surface velocity, and W is the particle velocity, the subscript 1 indicating
initial conditions before passage of the shock wave. Equation (3) expresses the
fact that the particle velocity in the shock at a free surface is approximately
twice the particle velocity in the shock in the medium in question.

The method used for determining the shock-parameter data for water and some
of the data for lucite consisted of simultaneous measurements of the shock vel-
ocity immediately inside the free surface and the free surface velocity as the
shock emerged from the water or lucite. Observations of the shock and free
surface velocities were made with a rotating mirror streak camera using diffuse
backlighting from an explosive flash bomb to show the propagation of the shock
wave and the free surface. Fig. 1 illustrates the aquarium setup. Note that
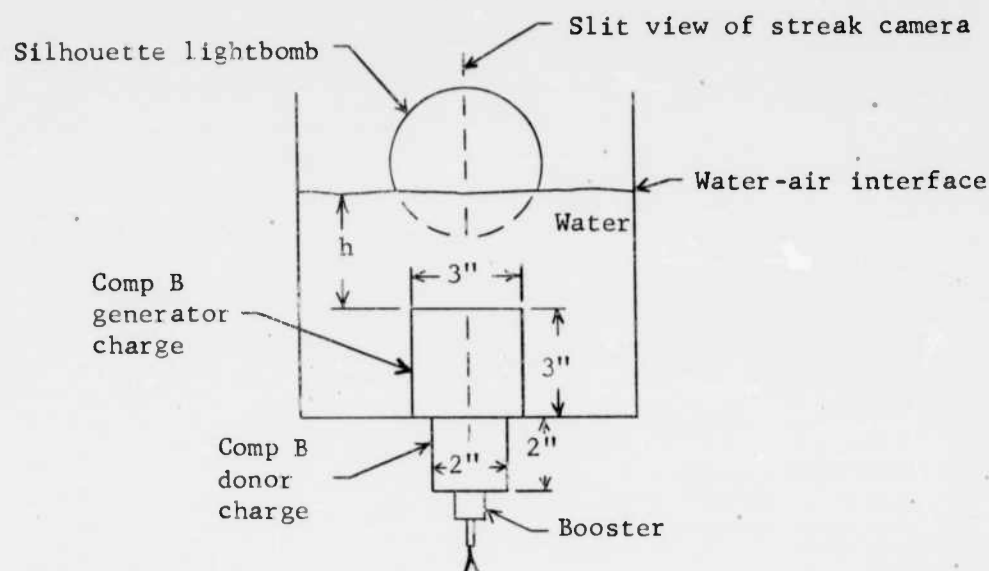
-5-

Fig. 1: Aquarium setup for measuring velocity of water shock along the charge
axis and free surface velocity.

point-initiated charges were used. For this reason it was necessary that the
slit view of the streak camera lie along the charge axis in order to obtain
the correct values of shock velocity and the corresponding free surface velocity.
Care was also taken in the alignment for the free surface in the cases of both
the water and the lucite to lie on the optic axis of the system so that the view
of the camera was flush with the free surface.

Two sizes of aquaria were used, the smaller being 6" x 6" x 6" and the larger
12" x 12" x 8", the size of the aquarium being dictated by the height, h, of
water above the receptor charge. As h was increased above a certain limit the
dimensions of the aquarium had to be increased due to the fact that the shatter-
ing of the glass propagated with a velocity which exceeded the shock velocity
in the liquid. Increasing the size of the aquarium, of course, resulted in an
increased path length for fracture which permitted the events of interest at the
water-air interface to be photographed before they were obscured.

The pressure or velocity of the shock wave when it reached the air surface was varied primarily by one of two methods: (1) by varying the height, h, of the liquid above the surface of the generator charge, and (2) by varying the size of the shock-generator charge, since use of smaller diameter generator charges resulted in a more rapid attenuation of the shock in water. With 3" diameter x 3" length shock-generator charges and 2" diameter x 2" length donor charges of Composition B the pressure of the shock wave, when it reached the water-air interface, could be varied conveniently between an upper limit of about 130 kb when the height of the liquid was 0.5 cm and a lower limit of about 30 kb using a liquid height of about 7 cm. For lower pressure, rather than employing further increases of water height, it was more convenient to reduce the size of the charge. Consequently, for pressures below roughly 30 kb and down to as low as 1 kb, 1" diameter x 1" length Composition B shock-generator charges and 1" diameter x 3" length donor charges were used. The calibration curve was extended to 155 kb by using a charge based on HMX as the shock-generator charge. This value was sufficiently high for measurements of detonation pressures of the explosives of interest. Walsh and Rice reported, however, extending shock parameter data to above 300 kb by hurling an explosively driven, thin, flat plate across a short air gap.

The silhouette-type lightbomb comprised a 4" diameter x 3" length 50/50 TNT/Composition B charge inserted in a 4" x 30" pasteboard tube of about 1/16" wall thickness. A sheet of translucent polyethylene plastic was taped to the front of the tube which served as a diffusing screen. The height of the light-bomb was adjusted so that the surface of the water in the aquarium was approximately in line with the center of the front of the lightbomb as viewed by the camera. The aquarium assembly and the streak camera were arranged such that the slit view of the streak camera was as shown in Fig. 1, i.e., perpendicular to the water-air interface and lying along the axis of the generator charge. Consequently, with proper synchronization of the lightbomb, a streak camera trace was obtained of the shock propagating through the liquid to the water-air interface. When the shock front reached the surface of the water the trace showed a rarefaction wave propagating back into the water and the spalling of the water surface. This

spall apparently is in the form of a very fine spray because it is relatively opaque and permits photographing the motion of its front and thus the direct recording of the free surface velocity.

Fig. 2 reproduces a typical streak camera trace showing the attenuating shock wave, the release wave, and spall. Note that the spall velocity is very constant. The results of interest obtained from the films are the shock velocity just as the shock reached the interface and the free surface or spall velocity. Both these measurements were obtained from the slopes of the traces at the interface through application of the proper magnification factors and camera writing speed. The writing speed of the camera in general was chosen such that the slopes of the shock wave trace and the free surface trace about equally bracketed the slope corresponding to a 45° angle.

The water used in this investigation was ordinary tap water rather than distilled water because the amounts required were rather large (some aquaria holding seven gallons) and the difference between the compressibility of distilled water and tap water is small. The temperature of the water was $20°C \pm 5C°$.

A few shock-parameter determinations for lucite were made in the same manner as those for water, i.e., by simultaneous measurements of shock velocity at the free surface and the free surface velocity. However, a greater number of determinations were made by transmitting the shock from lucite into water, measuring the final velocity of the shock in lucite and the initial velocity of the shock in water by means of a streak camera (utilizing a silhouette backlight bomb to render the shocks visible), and then by means of the previously obtained equation of state for water and equation (1), calculating the shock pressure in lucite immediately inside the lucite-water interface. The shocks in lucite were generated by the detonation of 4.8 cm diameter x 18 cm length, point initiated, cylindrical Composition B charges. As in the aquarium method the assemblies were carefully aligned in order that the slit view of the streak camera fell along the charge axis which made the use of expensive plane wave initiators unnecessary. The strength of the shock in lucite at the lucite-water interface was regulated by varying the thickness of lucite between the charge and the water. The diameter of the lucite was in all cases sufficiently large to

-8-
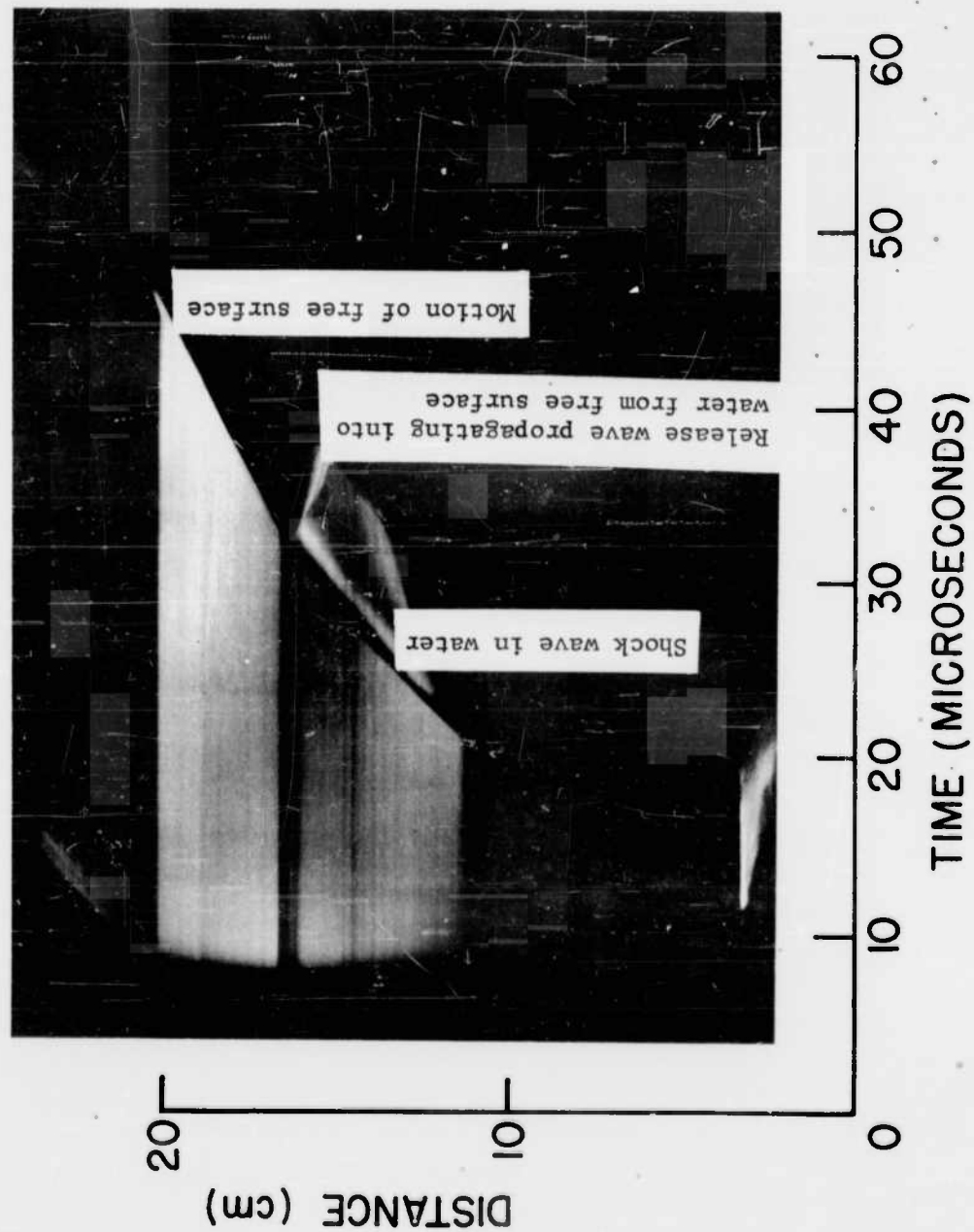
Fig. 2: Typical streak camera trace obtained using the arrangement
of Fig. 1 (shock parameter determination for water).

shield the detonation products from the region where the motion of the shock wave was observed.

    b. <u>Detonation pressure determinations</u>

    Fig. 3 illustrates the aquarium assembly used for measuring the initial velocity of the shock (and pressure) in water transmitted directly from a detonation wave. As in the previous cases the assembly was aligned such that the streak camera observations were made along the charge axis, the height and tilt of the assembly being such that the bottom face of the charge in this case was coincident with (and parallel) to the optical axis of the camera. The streak camera at this installation viewed upward through a periscope in which the line of sight was reflected to a horizontal direction by a front surface mirror. The camera was mounted on a turntable and three supporting casters, permitting rotation of the camera about its optical axis. Thus, the slit view of the camera could conveniently be adjusted to either the horizontal or vertical direction or to any position between them simply by rotation of the turntable.

Fig. 3: Aquarium assembly for measurement of velocity along the axis (and pressure) of the transmitted shock in water from a detonation wave.

This method of mounting the camera therefore permitted the proper alignment to be made with ease.
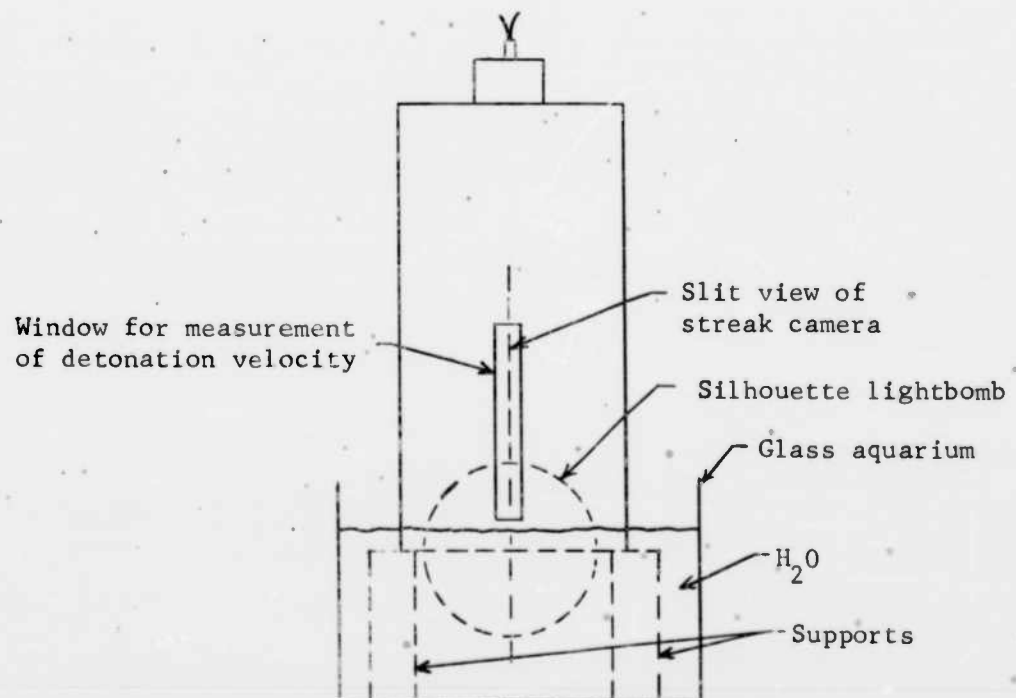
The cast charges were detonated with the bare end immersed in the aquarium. However, in cases where there existed the possibility of absorption of water or solution of some of the charge components the charges were sprayed with Krylon for waterproofing. Charges made up from granular or loose material were vibrator-packed in thin-walled (approximately 1/16" thick) cardboard tubes. The ends of the charges which were immersed in water in these cases were "closed off" with a layer of polyethylene 3 mils thick which was too thin to affect appreciably the shock transmitted into the water.

The average densities of all charges were determined just prior to firing. In addition to the determination of the initial velocity of the shock transmitted into water the detonation rate of the charge was measured, and thus all variables were evaluated whose magnitudes were required in the impedance mismatch equation for calculation of pressure in the incident medium in terms of that in the transmission medium. Detonation velocities as well as the initial shock velocities were calculated from the slopes of the traces. This procedure when carefully applied was found to yield satisfactory results even for the initial shock velocity determinations because care was taken to obtain traces of approximately 45° slope but more importantly because in many cases (with the primary exception of short charges) the attenuation of the water shock during the initial stages proved not to be rapid.

Numerous measurements of the peak pressure in the detonation wave to detect pressures higher than the C-J pressure have been carried out previously.[13,14] However, these experiments utilized measurements of free surface velocity of an aluminum plate in contact with the test explosive. Since the observations were carried out on the free surface or exit side of the aluminum rather than at the explosive-metal interface, extrapolations to zero thickness had to be made in order to determine the pressure or particle velocity at the detonation front. The fact that extrapolations were required dictated the use of very thin plates for which questions as to the validity of the measurements have been raised.[15,16]

The difficulties in using excessively thin plates in the method of Ref. 13 and 14 were amplified by the fact that experiments were devoted mainly to

explosives of short reaction zone length, such as Composition B, cast TNT, and fine, granular TNT for which the detonation "spike" would be "erased" quickly as it propagated into the aluminum. In the aquarium method, however, where a continuous observation of the shock wave velocity from the explosive-water interface outward into the liquid is possible, one does not need to use thin layers of the transmitting medium. Admittedly, a streak camera may not be able to resolve very rapid changes in velocity (or pressure) in a short distance near the explosive-water interface. Consequently, in this study emphasis was placed upon the use of explosives known to possess long reaction zone lengths and especially those whose characteristic impedances very nearly equalled the shock impedance of water, thus assuring that the impedance mismatch equation represented a good approximation for the pressure in the explosive and that conditions in the reaction zone would not be altered to any appreciable extent by compression or rarefaction waves reflected from the explosive-water interface.

The explosives included in this study were pelleted TNT of standard Tyler mesh sizes, -4+6, -6+8, -8+10, -48+65 granular TNT; loose packed 50/50 NH_4NO_3/ TNT; and cast 50/50 amatol. Also included here are measurements made by Bauer[17] for the "blasting agents", 94/6 AN/fuel oil and the coarse TNT and Composition B "slurries",[18] because the reaction zone lengths of blasting agents are quite likely among the longest of all detonating explosives. Also additional measurements are included for explosives of much shorter reaction zone length, namely granular RDX, granular RDX-salt, cast TNT, cast 65/35 baratol, 50/50 pentolite, Composition B, HBX-1, and a special explosive X. Measurements of this type were presented previously for pentolite, Composition B, TNT and tetryl by Cook, Pack and McEwan[16] and are included here for completeness.

Except for a study with Composition B and one with a special explosive X where charge length was varied to observe transient effects of pressure vs charge length the charge lengths used in this investigation were all at least four charge diameters in order to insure that the detonation velocity was constant before the detonation front reached the end of the charge. In the case of the pelleted TNT and the blasting agents, all of which possessed long reaction zone lengths, the charge diameters were varied between values extending in some cases from the critical diameter to a diameter sufficiently large for the detonation velocity to be nearly ideal.

Results

(a) Shock parameter determinations

Table I presents the experimental shock velocity, free surface velocity, particle velocity ($W \doteq V_{fs}/2$) and pressure results for water. In Fig. 4 are plotted the experimental points with pressure as the ordinate and shock velocity as the abscissa. Fig. 5 presents a similar plot in which the low pressure part of the curve of Fig. 4 has been expanded to a larger scale. On both figures the smooth curve through the points represents an approximate best fit as "drawn by eye" to the data. Velocity-pressure values from this curve of best fit are given in Table II and represent the most reliable values.

Results of Snay and Rosenbaum,[8] and Walsh and Rice[11] also are plotted in Fig. 4. Note that Snay and Rosenbaum's results agree with the results of the present study at pressures up to about 10 kb, and from thence there is a tendency for their data to bear to the left showing that their results indicate a greater compressibility. The results of Walsh and Rice fall about midway between those of Snay and Rosenbaum and this study. The differences in compression between the results of Walsh and Rice, which should be more comprehensive than Snay and Rosenbaum's data, and the data of this study were 3.2% for a shock velocity in water of 3500 m/sec and 2.8% for a shock velocity of 5500 m/sec, corresponding to pressures of 31 kb and 125 kb, respectively. The disagreement in pressures at these two velocities amounts to 9.7% for the lower velocity and 4.2% for the higher one.

The agreement between the shock parameter data for water obtained by Walsh and Rice and the data of this investigation is reasonably good. One may conclude, therefore, that the Rankine Hugoniot curves for water are now known with sufficient accuracy that water may reliably be used as the transmission medium for the measurement of pressures in shock and detonation waves.

In Table III are listed shock-parameter results for lucite in the form of shock velocity vs shock pressure, the data being portrayed graphically in Fig. 6. No differentiation was made in either case as to which of the two methods was used to obtain a given $p(V)$ point because the results of the two methods were indistinguishable within the limits of the experimental error involved. The smoothed results representing the most reliable values are given in Table IV.

Table I: Experimental shock parameter data for water (20°C $\pm$ 5C°)

Shot No.*	Shock Velocity (m/sec)	Free Surface Velocity (m/sec)	Particle Velocity (m/sec)	Shock Pressure (kilobars)
170	1630	143	72	1.16
182	1710	229	115	1.96
167	1810	355	178	3.21
168	1890	377	189	3.57
178	1780	360	180	3.20
179	1820	368	184	3.35
169	2050	556	278	5.70
177	2070	550	275	5.69
176	2110	605	303	6.38
29	2410	940	470	11.3
40	2260	900	450	10.2
41	2300	920	460	10.6
174	2800	1010	505	14.1
175	2760	1020	510	14.1
171	3540	1600	800	28.3
199	3510	1780	890	31.2
21	3680	1740	870	32.0
187	4000	2150	1080	43.0
6	4330	2760	1380	59.8
19	4240	2830	1420	60.0
193	4250	3160	1580	67.2
195	4490	3080	1540	69.1
194	4750	3130	1570	74.3
196	4720	3040	1520	71.7
5	4650	3160	1580	73.5
13	4810	3310	1660	79.6
32	4610	3080	1540	70.9
201	4930	3230	1620	79.6
202	4750	3230	1620	77.8
203	4750	3280	1640	77.9
17	4680	3420	1710	80.0
30	4900	3290	1650	80.6
204	5070	3540	1770	89.7
205	4900	3560	1780	87.2
206	4900	3570	1790	87.5
207	4870	3540	1770	86.2
200	4810	3380	1690	81.2
18	4960	3800	1900	94.2
16	5070	3840	1920	97.3

* Note: Shot number has been included for convenience of the writers.

Table I: Continued

Shot No.	Shock Velocity (m/sec)	Free Surface Velocity (m/sec)	Particle Velocity (m/sec)	Shock Pressure (kilobars)
4	5080	3850	1930	98
190	5070	4200	2100	106
11	5470	4100	2050	112
189	5380	4210	2110	113
192	5530	4120	2060	114
213	5570	4110	2060	114
1	5480	4690	2350	128
2	5580	4440	2220	124
3	5320	4500	2250	120
10	5610	4400	2200	123
36	5420	4440	2220	120
37	5330	4490	2250	120
38	5410	4530	2270	122
34	5660	4730	2370	134
9	6050	4720	2360	143
183	6010	5040	2520	151
181	6130	4980	2490	153
184	6270	5090	2550	160
185	6200	5150	2580	160
186	6290	4980	2490	157

Table II: Smoothed shock parameter results for water ($20°C \pm 5C°$)

Shock Velocity (m/sec)	Shock Pressure (kilobars)	Shock Velocity (m/sec)	Shock Pressure (kilobars)
1450	Sonic	3450	30.0
1620	1.0	3820	40.0
1740	2.0	4120	50.0
1840	3.0	4350	60.0
1940	4.0	4570	70.0
2020	5.0	4780	80.0
2100	6.0	4980	90.0
2170	7.0	5170	100.0
2240	8.0	5350	110.0
2310	9.0	5530	120.0
2380	10.0	5700	130.0
2680	15.0	5870	140.0
2980	20.0	6040	150.0
		6200	160.0
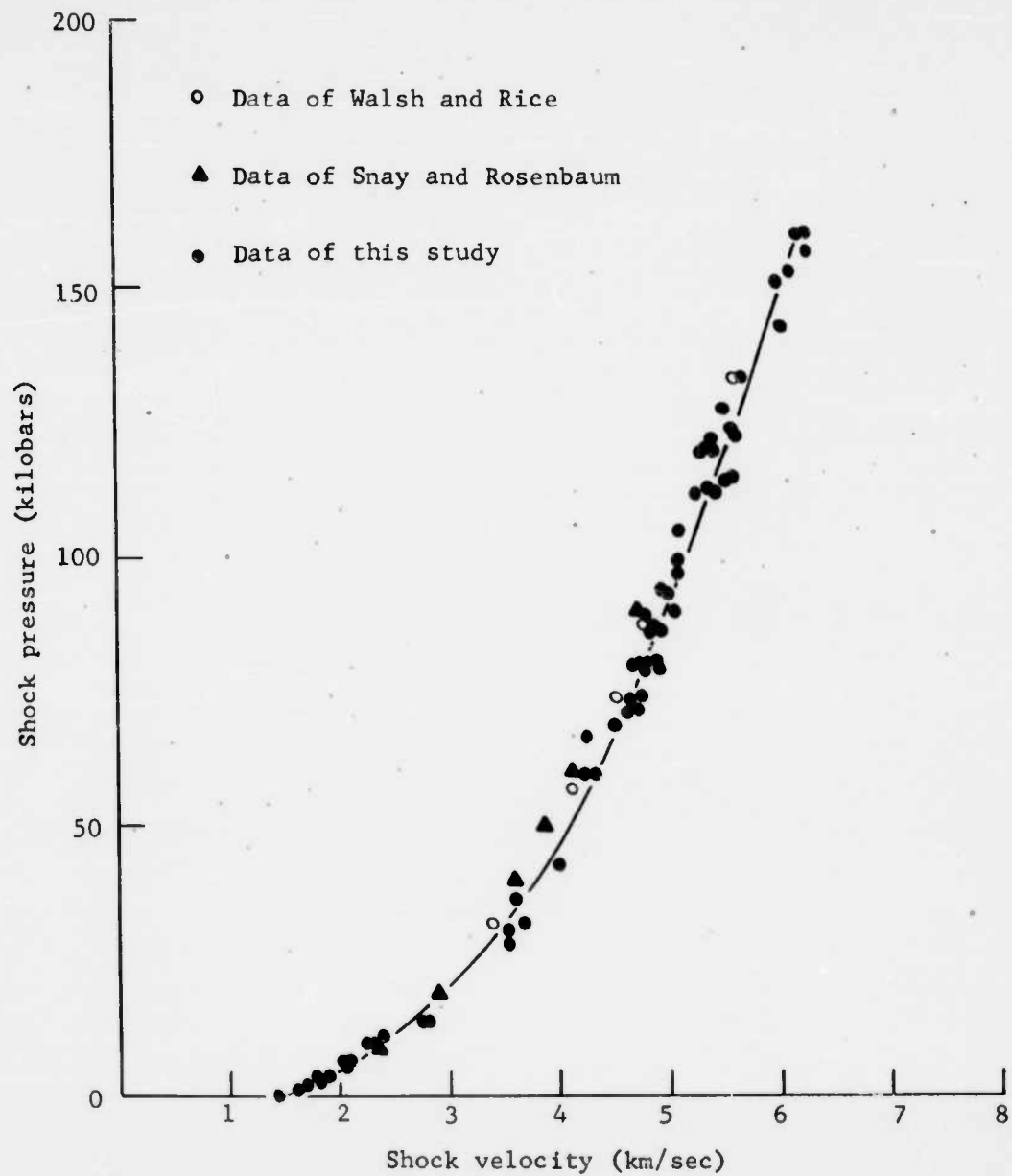
Fig. 4: Experimental shock velocity vs pressure data for water.
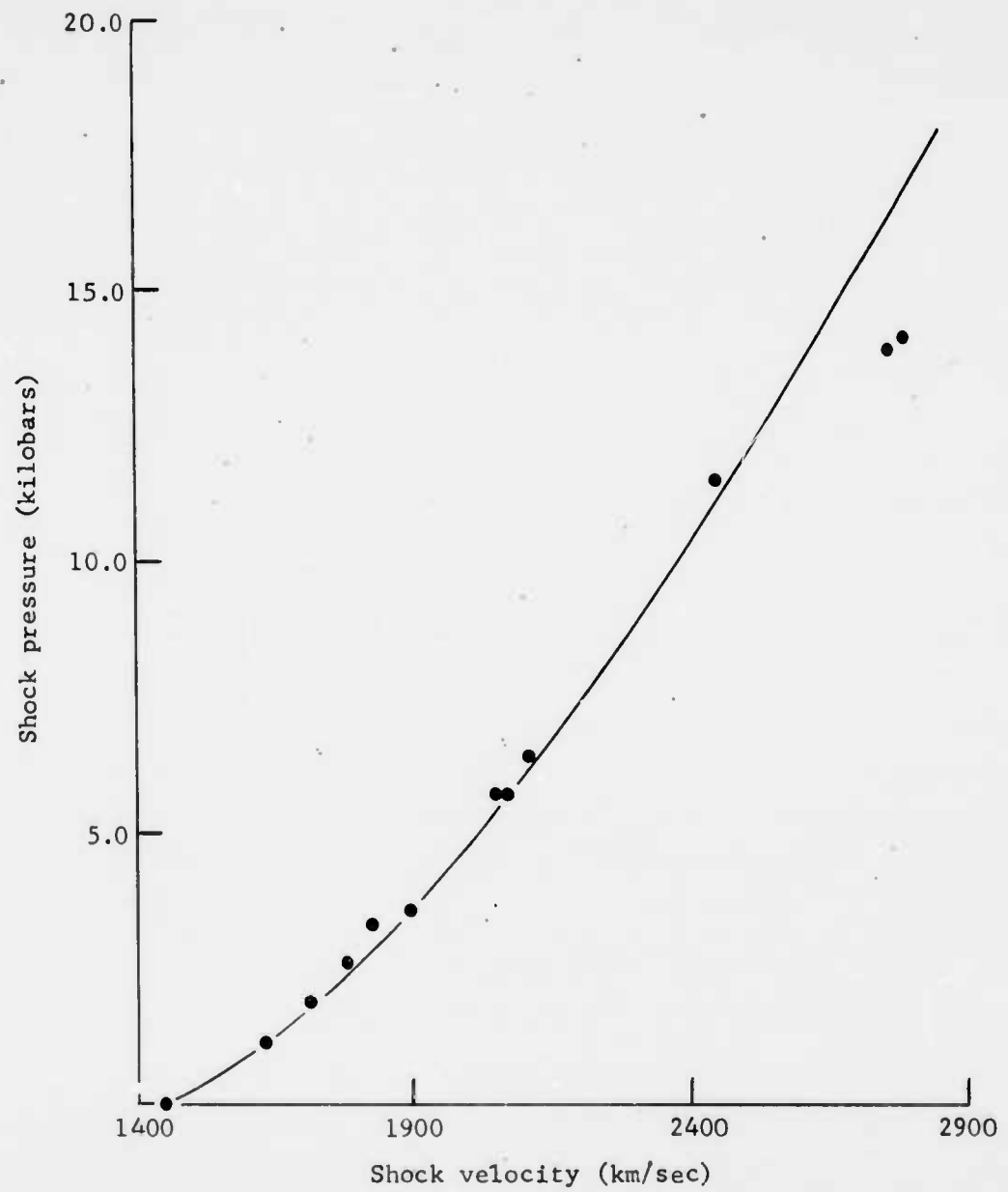
Fig. 5: Experimental shock velocity vs pressure data for water (low pressures).

Table III: Experimental shock parameter data for lucite

Shock Velocity (m/sec)	Shock Pressure (kilobars)	Shock Velocity (m/sec)	Shock Pressure (kilobars)
3300	19	4000	33
3400	23	4000	35
3520	23	4400	48
3700	27	4620	59
3740	29	5370	105
3800	30	6040	134
3800	31	6200	166
3950	32	6360	169

Table IV: Smoothed shock parameter data for lucite

Shock Velocity (m/sec)	Shock Pressure (kilobars)	Shock Velocity (m/sec)	Shock Pressure (kilobars)
3350	20	5410	100
3820	30	5560	110
4160	40	5700	120
4430	50	5840	130
4670	60	5960	140
4880	70	6100	150
5070	80	6210	160
5250	90	6330	170

-18-

Fig. 6:   Experimental shock velocity vs pressure data for lucite.

Note that in Fig. 6 the curve was not extended to the sonic velocity because it was found that considerable variation existed in values of sonic velocity available for lucite, and thus the true value was uncertain.

(b) Detonation pressure measurements

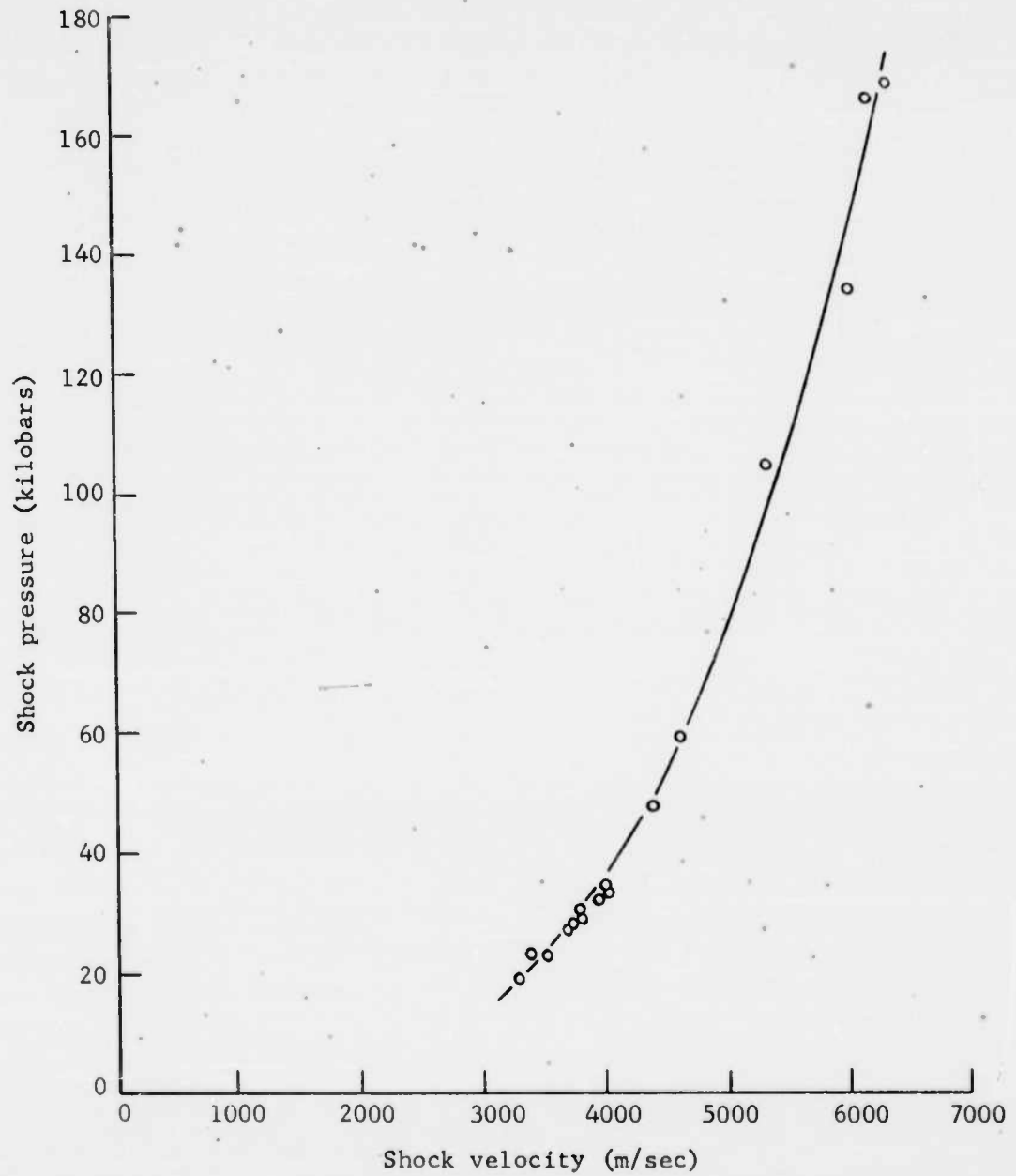Results obtained for the military-type explosives in which the charge length was maintained at approximately 4 diameters to assure that the detonation wave was steady are listed in Table V. All the charges in this case may be considered to be unconfined, the cast charges being bare and the loose charges being contained in 1/16" thick pasteboard tubing. In Table V are listed the type explosive, the charge density, the charge diameter, the measured detonation velocity (D), the initial velocity of the shock transmitted into water (V_t), the initial pressure of the shock front in water (p_t), the ideal or hydrodynamic velocity D^* corresponding to the given density, the pressure of the detonation wave or incident wave (p_i) calculated through application of equation (1) (the impedance mismatch equation), the ideal detonation pressure calculated by means of thermohydrodynamic theory as outlined in Ref. 19, the ratio of pressure of the incident wave or detonation wave to ideal detonation pressure, and the $(D/D^*)^2$ ratio. Table VI lists similar data for loose-packed 50/50 AN/TNT mixtures which, similar to coarse TNT, represents another explosive of long reaction zone length.

Fig. 7 presents results for special explosive X in 5 cm diameter and Composition B in 4.8 cm diameter for which the charge length was varied from 1 cm to 6 cm to determine if a pressure-buildup effect existed in explosives of very short reaction zone lengths where one would expect no detonation velocity transient. These charges were all boostered with identical 1/2" x 1" pressed RDX boosters. With such short charges, however, difficulty was encountered in measuring the initial velocity of the shock wave in water because of a rapid attenuation in velocity of the shock in the aquarium. The plot of the results indicates, despite the observed scatter, a small pickup in detonation pressure as the charge length was increased. Whether or not the detonation velocity increased slightly over this region in order to produce the pressure pickup was not determined.

-20-

Table V: Experimertal pressure measurement results for military type explosives

Explosive	ρ_1 (gm/cm³)	d_{exp} (cm)	D (m/sec)	V_t (m/sec)	P_t (kb)	D* (m/sec)	P_i (kb)	P_2* (kb)	P_i/P_2*	$(D/D*)^2$
RDX	1.10	1.25	5830	4640	75	6400	89	115	.78	.91
RDX	1.23	2.53	6410	5250	108	6850	135	145	.93	.90
RDX	1.17	2.53	6360	4760	80	6660	103	130	.79	.90
RDX	1.22	2.53	6535	5520	120	6830	147	142	1.02	.93
RDX	1.21	2.53	6610	5470	115	6800	141	139	1.01	.94
RDX	1.18	3.77	6750	4920	89	6730	118	130	.91	1.00
RDX	1.21	4.40	6665	5010	94	6800	123	139	.90	.96
RDX	1.21	5.05	6825	5325	113	6800	143	139	1.04	1.01
RDX	1.17	5.05	6750	5270	105	6670	131	130	1.01	1.00
RDX	1.17	5.05	6730	5400	112	6670	138	130	1.07	1.02
RDX	1.10	6.30	6400	5085	94	6370	112	115	.98	1.00
RDX	1.13	7.62	6620	5115	97	6550	119	122	.98	1.02
65/35 Ba(NO₃)₂ TNT	2.35	5.00	5150	4420	62	5600	116	156*	.74	.85
HBX-1	1.75	5.00	7160	5485	116	7400	190	190*	1.00	.94
50/50 NH₄NO₃ TNT (AN #1)**	1.58	4.80	5720	4860	84	6600	120	144	.84	.76
50/50 NH₄NO₃ TNT (AN #2)**	1.53	4.80	5550	4610	72	6450	102	136	.75	.74
50/50 NH₄NO₃ TNT (AN #1)**	1.58	7.62	6230	5160	100	6600	145	144	1.00	.89
50/50 NH₄NO₃ TNT (AN #2)**	1.53	7.62	6040	4850	85	6450	121	136	.89	.94
80/20 RDX NaCl	1.32	2.53	5790	4850	85	6310	110	125	.88	.85
80/20 RDX NaCl	1.30	4.40	6198	4925	87	6240	115	121	.95	.98
80/20 RDX NaCl	1.28	5.00	6198	5000	92	6180	119	118	1.01	1.01
TNT -8+10 mesh	.95	5.05	3670	3810	40	4850	38	62	.61	.58
TNT -8+10 mesh	.95	5.05	3790	3906	43	4850	41.5	62	.67	.61
TNT -8+10 mesh	.97	7.62	4630	4080	49	4920	52	64	.81	.69
TNT -8+10 mesh	1.01	7.62	4660	4395	62	5050	64	70	.91	.85
TNT -8+10 mesh	1.00	7.62	4711	4220	56	5010	59	68	.87	.38
TNT -8+10 mesh	.99	10.00	4765	4410	63	4960	65	66	.98	.92
TNT -8+10 mesh	1.01	10.00	4835	4272	58	5060	62.5	70	.88	.92

Table V: Continued

Explosive	ρ_1 (gm/cm³)	d_{exp} (cm)	D (m/sec)	V_t (m/sec)	P_t (kb)	D* (m/sec)	P_i (kb)	P_2^* (kb)	P_i/P_2^*	$(D/D^*)^2$
TNT -6+8 mesh	1.00	7.62	4505	4410	63	5010	64	68	.94	.81
TNT -6+8 mesh	.99	7.62	4507	4000	47	4980	50	67	.75	.82
TNT -6+8 mesh	1.01	10.00	4675	4420	63	5060	65	70	.93	.85
TNT -6+8 mesh	1.02	10.00	4966	4362	61	5100	66	72	.92	.96
TNT -6+8 mesh	.97	16.10	4880	4350	60	4880	63	63	1.00	1.00
TNT -4+6 mesh	1.00	7.62	4414	3865	43	5010	45.5	68	.67	.77
TNT -4+6 mesh	1.02	10.00	4669	4206	55	5090	59	72	.82	.85
TNT -4+6 mesh	1.01	10.00	4645	4365	60	5030	62	68	.91	.85
TNT -4+6 mesh	1.06	12.35	4995	4410	63	5200	69	77	.90	.92
TNT -4+6 mesh	1.00	15.90	4800	4480	65	5010	66	68	.96	.92
TNT -4+6 mesh	0.99	20.30	5030	4350	58	4980	62	67	.93	1.02
TNT -4+6 mesh	0.98	20.30	5050	4180	53	4950	58	66	.88	1.04
TNT -4+6 mesh	0.98	20.30	4930	4130	49	4950	53	66	.80	.99
TNT -4+6 mesh	1.00	20.30	5040	4340	57	5010	62	68	.91	1.01
TNT -4+6 mesh	.99	25.30	4600	4425	64	4980	65	67	.97	.97
TNT -48+65 mesh	.80	2.53	3840	4075	49	4350	43	46	.93	.77
TNT -48+65 mesh	.87	2.53	3870	4080	49	4600	45	52	.86	.72
TNT -48+65 mesh	.86	3.77	4550	4045	47.5	4550	47	51	.92	.93
TNT -48+65 mesh	.87	3.80	4445	4225	54	4650	52	52	1.00	.93
TNT -48+65 mesh	.86	4.40	4385	4080	49	4550	47	51	.92	.93
TNT -48+65 mesh	.87	5.05	4550	4385	62	4550	59	52	1.00	1.10
TNT -48+65 mesh	.87	5.05	4580	4262	56	4600	54	52	1.00	1.04
TNT -48+65 mesh	.91	5.05	4430	3910	45	4750	46	57	.81	.86
TNT -48+65 mesh	.91	5.05	4680	3910	45	4750	47	57	.82	.96
TNT -48+65 mesh	.81	7.62	4400	3915	43	4350	41	46	.89	1.00
TNT -48+65 mesh	.86	7.60	4525	4400	62	4540	57	51	1.11	.99
Composition B***	1.71			5800	140		230	230	1.00	
50/50 Pentolite ***	1.65			5680	134		214	215	.995	
Tetryl***	1.50			5400	115		172	175	.982	
TNT***	1.58			5100	96		159	160	.994	
TNT***	.87			3600	34		37	42	.881	

Table V: Continued

*   Computed from $p_2^* = (\rho D^2)/4$

**   AN #2 $\doteq$ 35 mesh
     AN #1 was somewhat finer

*** Data from Ref. 16 (Detonation velocities were not measured. However, Composition B, 50/50 pentolite, pressed tetryl, and cast TNT should have propagated at ideal velocity).

ρ = average density of the explosive

D = measured detonation velocity

D^* = ideal or hydrodynamic value of detonation velocity

V_t = initial velocity of shock wave in the transmitted medium (water)

p_t = initial pressure of the shock wave in the transmitted medium (water)

p_i = pressure of the wave in the incident medium (the explosive) calculated from the impedance mismatch equation in terms of p_t

p_2^* = Chapman-Jouguet value of the detonation pressure at ideal detonation velocity calculated from thermohydrodynamics

-23-

Table VI: Experimental pressure measurements for loose-packed 50/50 AN/TNT

d (cm)	ρ_1 (g/cm^3)	D (m/sec)	P_t (kbar)	P_i (kbar)	P_i/P_2^*(1)	P_i/P_2^*(2)	$(D/D^*)^2$	No. of Shots
2.54	0.96	2910	23.5	22	0.42	0.33	0.36	1
2.54	0.95	2830	22	21	0.39	0.32	0.34	1
2.54	1.00	3170	31	30	0.53	0.41	0.40	1
3.81	0.97	3600	44	42	0.74	0.62	0.53	1
3.81	0.97	3630	34	34	0.60	0.50	0.55	1
3.81	0.98	3680	37	36	0.64	0.52	0.55	1
5.04	0.98	4080	48	48	0.85	0.67	0.66	5
10.00	0.96	4570	61	62	1.14	0.91	0.86	7
15.20	0.96	4760	67	67	1.24	1.00	0.95	6
20.4	0.96	4800	67	68	1.33	1.00	0.96	2
25.4	0.94	4880	69	69	1.29	1.08	1.00	4

ρ_1 = bulk density of explosive

D = measured detonation velocity

D* = ideal or hydrodynamic value of detonation velocity

P_t = initial pressure of the shock wave in the transmitted medium (water)

P_i = pressure of wave in the incident medium (explosive) calculated from the impedance mismatch equation

P_2^* = Chapman-Jouguet value of the detonation pressure at ideal detonation velocity calculated from thermohydrodynamic theory. (P_i/P_2^* are listed using the results of two thermohydrodynamic calculations that were available but which were not in agreement)
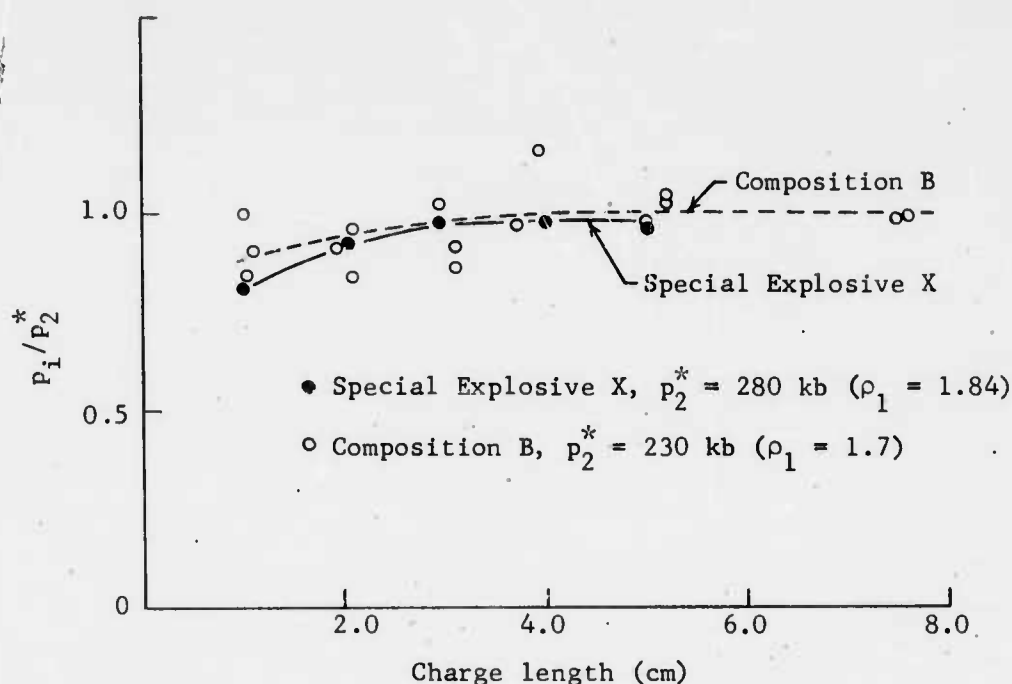
Fig. 7: Pressure of the detonation wave (measured by the aquarium technique) as a function of charge length for 5 cm diameter special explosive X and 4.8 cm diameter Composition B boostered with 1/2" x 1" pressed RDX.

Data for the commercial blasting agents are given in Table VII through the courtesy of the Intermountain Research and Engineering Company, Salt Lake City, Utah. These results are given both for unconfined charges and charges confined in 3/8" thick or 1/4" thick steel tubing. One will note that the detonation velocity and pressure of the low density AN/fuel oil mix was very sensitive to confinement. In 5" diameter unconfined charges the detonation velocity was only 2770 m/sec which corresponded to a D/D* ratio of only 0.66 while with 3/8" steel confinement in the same diameter the detonation velocity was 3930 m/sec corresponding to a D/D* ratio of 0.94. The DBA series of coarse TNT or Composition B "slurries" were much less sensitive to confinement probably because the detonation pressure is much higher.

In comparing the measured values given in Table V for pressure in the explosive, that is, pressure in the incident waves (p_i) obtained by the aquarium technique with the Chapman-Jouguet value of the detonation pressures

-25-

Table VII: Experimental pressure measurement results for commercial blasting agents

Blasting Agent	ρ (g/cm³)	d (in)	Confinement	No. of Measurements	D (m/sec)	V_t (m/sec)	P_t (kb)	D* (m/sec)	P_i (kb)	P_2^* (kb)	P_i/P_2^*	$(D/D^*)^2$
94/6 AN/FO	0.82	5	None	3	2770±50	2550±70	12±.5	4200	13.5±1.0	40	0.34	0.43
94/6 AN/FO	0.82	5	Steel*	2	3930±20	3900±170	42.5±3	4200	37.5±1.5	40	0.93	0.88
DBA-1	1.52	5	None	5	4900±100	4000±100	46±3	6400	85±3	150	0.57	0.59
DBA-1	1.52	5	Steel*	1	5120	4720	77	6400	103	150	0.69	0.64
DBA-2	1.68	5	None	2	5500±100	4480±120	64±4	6800	97±5	180	0.54	0.66
DBA-2	1.50	5	Steel*	2	5270±70	4800±100	80±5	6500	111±10	155	0.71	0.66
DBA-3	1.58	5	None	4	5800±80	4600±200	71±10	6800	126±8	180	0.70	0.72
DBA-3	1.58	5	Steel*	2	6180±80	5530±190	125±10	6800	172±11	180	0.95	0.83
DBA-3	1.58	2	None	3	5300±100	4700±100	74±5	6800	101±5	180	0.56	0.63
DBA-3	1.58	2	Steel*	2	5885±15	5050±150	94±7	6800	134±6	180	0.75	0.75

* Steel confinement was 3/8" tubing for 5" diameter and 1/4" tubing for 2" diameter

ρ = average density of the explosive

D = measured detonation velocity

D* = ideal or hydrodynamic value of detonation velocity

V_t = initial velocity of shock wave in the transmitted medium (water)

P_t = initial pressure of the shock wave in the transmitted medium (water)

P_i = pressure of the wave in the incident medium (the explosive) calculated from the impedance mismatch equation in terms of P_t

P_2^* = Chapman-Jouguet value of the detonation pressure at ideal detonation velocity calculated from thermohydrodynamics

Note: The plus and minus variations cover the spread in the experimental data

calculated from thermohydrodynamic theory, one will note that in every case
where the detonation wave propagated at ideal velocity, p_i was found to agree
within experimental error with the calculated detonation pressure. A similar
result was found in the study of Ref. 12, data for which are given in Table
VII. Unfortunately, accurate thermohydrodynamic calculations were not
immediately available for the 50/50 AN/TNT mixtures in Table VI to provide
similar comparisons. However, with the experimental results listed in Table VI
are given for comparison the results from two rather old thermohydrodynamic
computations which are not in agreement. One will note that in terms of one
of the thermohydrodynamic calculations an overpressure of a few percent was
measured consistently for the detonation front with respect to the Chapman-
Jouguet pressure, while in comparison to the other calculation no overpressure
existed. This discrepancy could be resolved with an accurate thermohydrodynamic
calculation. However, it was considered beyond the realm of this study to
perform such a calculation.

It should be stressed that in the case of most of the loose-packed explosives
the impedance match between the explosive and water was very good. Therefore,
calculations of pressure in the incident medium in terms of pressure of the
transmitting medium, through application of the shock impedance mismatch equation,
should be very reliable. Furthermore, conditions in the reaction zone would not be
affected appreciably by reflected compression or rarefaction waves from the
explosive-water interface.

Since the pressure through a detonation wave is given by the relation
$p = \rho_1 DW$ one would expect that in non-ideal detonations the Chapman-Jouguet
pressure, which is defined as the pressure at the surface in the wave ahead
of which chemical reaction supports propagation and behind which chemical
reaction lends no support, should be given by

$$p \doteq (D/D*)^2 p_2^* \qquad (4)$$

where asterisks signify ideal values, p_2^* being the ideal detonation pressure.
Equation (4) assumes that W/D depends only on ρ_1 and not on $D/D*$, an assumption
well justified by the generality of the covolume-specific volume (α[v] curve
for high explosives).[19] Comparisons of $(D/D*)^2$ with p/p_2^* given in Tables
V, VI and VII indeed show a striking agreement in most cases.

Some very important information regarding the pressure or particle velocity profiles of detonation waves are apparent from this study. According to the Zeldovich-von Neumann concept, which is based upon transport phenomena being negligible in a detonation wave, the pressure at the detonation front should be approximately twice the Chapman-Jouguet pressure. Then as chemical reaction proceeds the pressure decays along the Rayleigh line to the Chapman Jouguet value at the end of the reaction zone. For explosives of reaction zone length of the order of a few mm or less, e.g., Composition B, the presence of the von Neumann spike would be very difficult to detect. As mentioned earlier previous experiments to determine the pressure profiles through reaction zones by means of the aluminum free surface velocity technique were devoted primarily to explosives of very short reaction zone length, i.e., Composition B. This choice of explosive necessitated the use of very thin plates for which the free surface velocity measurements were in question. Since there is no reason to believe that an overpressure, if present, would exist in a rapidly reacting explosive and not in a slowly reacting one, it would seem prudent to look for evidence of a spike in slowly reacting explosives. The blasting agents listed in Table VII represent a class of explosives known to possess the longest reaction zones of the detonating type explosives, and according to any published theory possess reaction zone lengths sufficiently great that a spike could easily be detected by the aquarium technique. The coarse TNT series, especially -4+6 mesh TNT, and the loose packed 50/50 AN/TNT series, also have reaction zone lengths which are ample for easy detection of a spike by the aquarium technique, yet no evidence of a spike overpressure was noted in any case (except a few percent for the 50/50 AN/TNT when comparisons were made to one of the thermo-hydrodynamic calculations).

Fig. 8 shows a streak camera trace illustrating the aquarium technique for measuring detonation pressures by transmitted shock waves in water. In this case the charge consisted of a slurry explosive detonated in a 5" I.D. steel tube. Note the slow attenuation of the velocity of the shock wave in water. This is typical of large charges and permits an accurate measurement of the initial velocity of the shock.
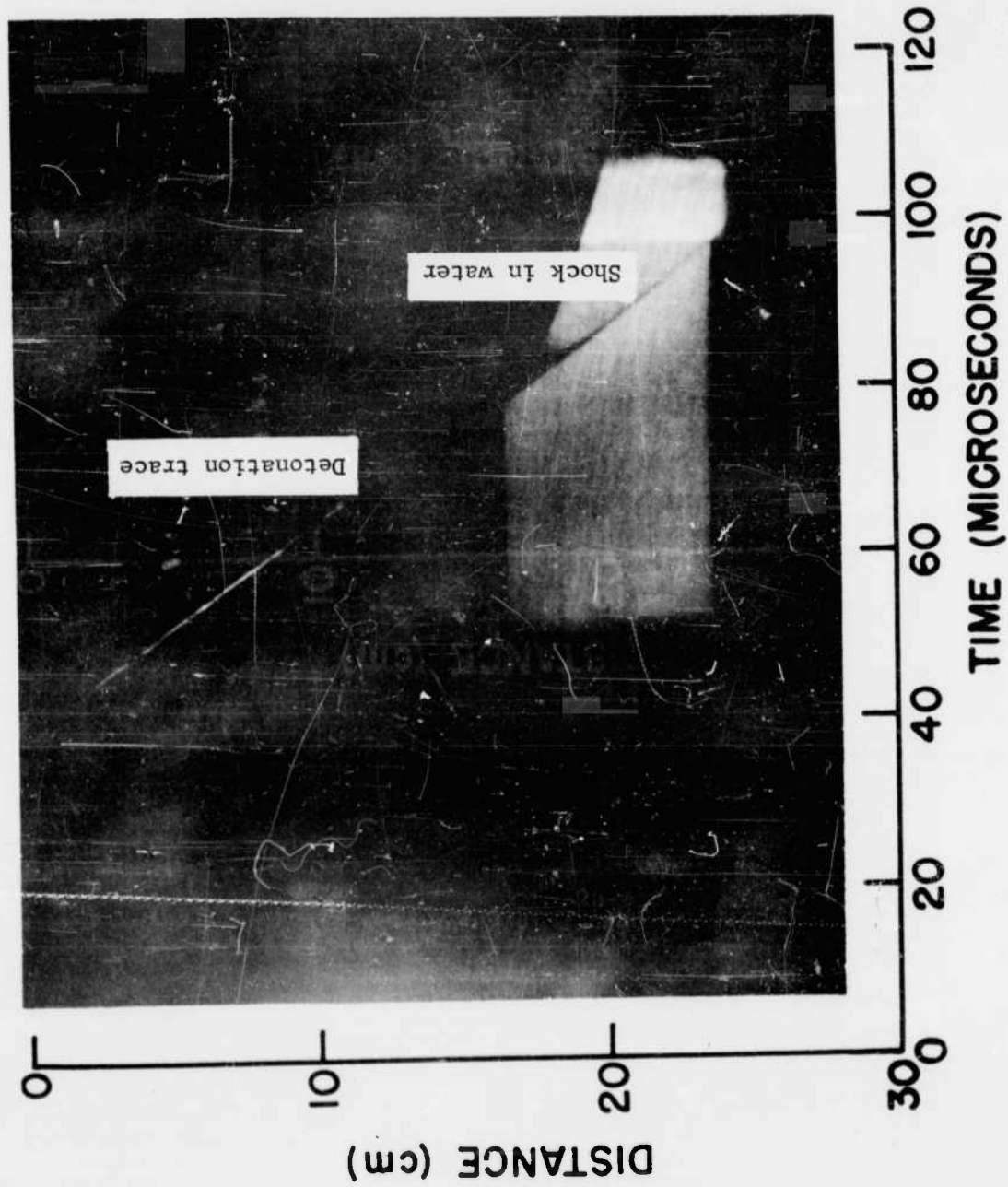
Fig. 8: Streak camera trace illustrating the aquarium technique for measurement of detonation pressure (explosive, slurry in 5" I.D. steel tube).

-29-

In conclusion, therefore, since even with explosives possessing the longest known reaction zone lengths, the aquarium technique measured the Chapman-Jouguet value of the detonation pressure, it appears that the highest pressure in the detonation wave is the Chapman-Jouguet pressure. This conclusion is strengthened by the fact that such results have been obtained for cases where the characteristic impedance of the explosive very nearly equalled the shock impedance of the water under which condition computations from the impedance mismatch equation would be expected to be very reliable and waves reflected from the explosive-water interface would be too small to affect measurably conditions within the reaction zone.

Acknowledgement

BIBLIOGRAPHY

1. J. G. Kirkwood and E. W. Montrall, "The Pressure Wave Produced by an Underwater Explosion II," OSRD No. 670, June 1942.

2. J. G. Kirkwood and J. M. Richardson, "The Pressure Wave Produced by an Underwater Explosion III," OSRD No. 813, August 1942.

3. J. M. Richardson, J. M. Arons, and R. R. Halverson, "Hydrodynamic Properties of Sea Water at the Front of a Shock Wave", J. Chem. Phys., 15, 785-794 (1947).

4. A. B. Arons and R. R. Halverson, "Calculations for Sea Water at the Shock Front", OSRD No. 6577, March 1946.

5. W. Doering and G. Burkhardt, "Contribution to the Theory of Detonation", HEC Accession List No. 60, Page 4, Bias Group.

6. P. W. Bridgman, "Water in the Liquid and Five Solid Forms under Pressure", Proc. American Academy of Arts and Sciences, 47, 441-558 (1912).

7. P. W. Bridgman, "The Phase Diagram of Water to 45,000 kg/cm^2", J. Chem. Phys., 5, 964-966 (1937).

8. H. G. Snay and J. H. Rosenbaum, "Shockwave Parameters in Fresh Water for Pressures up to 95 Kilobars", NAVORD Report 2383, U.S. Naval Ordnance Laboratory, White Oak, Maryland, April 1952.

9. P. W. Bridgman, "Freezing and Compressions to 50,000 kg/cm^2", J. Chem. Phys., 9, 794-797 (1941).

10. P. W. Bridgman, "Freezing Parameters and Compression of Twenty-One Substances to 50,000 kg/cm^2", Proc. American Academy of Arts and Sciences, 74, 399-424 (1942).

11. J. M. Walsh and M. H. Rice, "Dynamic Compression of Liquids from Measurements in Strong Shockwaves", J. Chem. Phys., 26, (1957).

12. W. C. Holton, "The Detonation Pressures in Explosives as Measured by Transmitted Shocks in Water", NAVORD 3968, U.S. Naval Ordnance Laboratory, White Oak, Maryland, 1 December 1954.

13. R. E. Duff and E. Houston, "Measurement of the Chapman-Jouguet Pressure and Reaction Zone Length in a Detonating High Explosive", Second ONR Symposium on Detonation, Washington, D. C., February 9-11, 1955, page 225.

14. H. D. Mallory and S. J. Jacobs, "The Detonation Zone in Condensed Explosives", Second ONR Symposium on Detonation, Washington, D. C., February 9-11, 1955, page 240.

15. R. B. Clay, M. A. Cook and R. T. Keyes, "Plate Velocities in the Impulse
     Loading by Detonation Waves", Preprint 9, Symposium on Shock Waves in
     Process Equipment, Annual Meeting, Chicago, Illinois, American Institute
     of Chemical Engineers, December 8-11, 1957.

16. M. A. Cook, D. H. Pack and W. S. McEwan, "Promotion of Shock Initiation of
     Detonation by Metallic Surfaces", Trans. Fara. Soc., 56, No. 451, Part 7,
     July 1960.

17. A. Bauer and M. A. Cook, "Observed Detonation Pressures of Blasting Agents",
     The Canadian Mining and Metallurgical Bulletin, 54, 585, 62-65, January 1961.

18. M. A. Cook and H. E. Farnam, U.S. Patent No. 2,930,685, March 29, 1960.

19. M. A. Cook, "The Science of High Explosives", Reinhold Publishing Corporation,
     New York (1958).

DISTRIBUTION LIST

No. of copies

	No. of copies
Chief	
Department of the Navy	
Bureau of Naval Weapons	
Washington 25, D. C.	
Attn: ReU3	5
ReS3	1

Chief of Naval Research
Department of the Navy
Washington, D. C.
Attn: Chemistry Branch — — — 1

Commander
Naval Ordnance Laboratory
White Oak
Silver Spring, Maryland
Attn: Library, Dr. S. J. Jacobs
Mr. A. D. Solem 3

Commander
Naval Ordnance Test Station
China Lake, Inyokern, California
Attn: Library 2

Commander
Naval Proving Ground
Dahlgren, Virginia
Attn: Physics Division 1

Commanding Officer
Picatinny Arsenal
Dover, New Jersey 2

Commanding Officer
Naval Mine Depot
Yorktown, Virginia
Attn: R and D Laboratory 1

Commanding Officer
Detroit Arsenal
Center Line, Michigan
Attn: Mr. C. B. Salter 1

Commanding Officer
Franford Arsenal
Philadelphia 37, Pennsylvania
Attn: Mr. H. S. Lipinski 1

Commanding Officer
Redstone Arsenal
Huntsville, Alabama
Attn: Technical Library
Mr. Wade Ewart 1

Director
Applied Physics Laboratory
Johns Hopkins University
Silver Spring, Maryland
VIA: Inspector of Naval Ordnance
Applied Physics Laboratory
Johns Hopkins University
8621 Georgia Avenue
Silver Spring, Maryland 2

Director, ASTIA
Document Service Center
Arlington Hall Station
Arlington 12, Virginia 10

Commanding General
Aberdeen Proving Ground
Aberdeen, Maryland 1

Director
Ballistic Research Laboratories
Aberdeen, Maryland 2

Office, Chief of Ordnance
Department of the Army
Research and Development Division
Washington, D. C.
Attn: ORDTB Ballistics Section 2

Arthur D. Little, Inc.
Cambridge 42, Massachusetts
Attn: Dr. G. R. Handrick
VIA: Inspector of Naval Material
495 Summer Street
Boston 10, Massachusetts 1

Carnegie Institute of Technology
Pittsburgh, Pennsylvania
Attn: Dr. E. M. Pugh
VIA: Inspector of Naval Material
      Old Post Office Building
      Pittsburgh 19, Pennsylvania   1

Canadian Army Staff
2450 Massachusetts Avenue, N.W.
Washington 8, D. C.
VIA: Bureau of Naval Weapons
      Department of the Navy
      Washington 25, D. C.
      Attn: Ad8 Re2c   2

Science and Technology Division
Library of Congress
Washington 25, D. C.
Attn: Dr. Clement Brown, Head
       Bibliograph Section   1

British Joint Services Mission
1800 K Street, N.W.
Washington 6, D. C.
Attn: Mr. John Gibson
VIA: Bureau of Naval Weapons
      Department of the Navy
      Washington 25, D. C.
      Attn: Ad8, Re2c   2

Aerojet-General Cor
Azusa, California
Attn: Mr. Guy C. T
       Explosive Ord
VIA: BuAer Represe
      6352 N. Irwin
      Azusa, Califor

National Northern Div
American Potash and C
P. O. Box 175
West Hanover, Massa
Attn: A. T. Wilson
VIA: Inspector of
      495 Summer S
      Boston 10, Ma